
Generative Modeling of Graphs via Joint Diffusion of Node and Edge Attributes

Nimrod Berman^{*†} Eitan Kosman[†] Dotan Di Castro[†] Omri Azencot^{*}

Abstract

Graph generation is integral to various engineering and scientific disciplines. Nevertheless, existing methodologies tend to overlook the generation of edge attributes. However, we identify critical applications where edge attributes are essential, making prior methods potentially unsuitable in such contexts. Moreover, while trivial adaptations are available, empirical investigations reveal their limited efficacy as they do not properly model the interplay among graph components. To address this, we propose a joint score-based model of nodes and edges for graph generation that considers all graph components. Our approach offers two key novelties: (i) node and edge attributes are combined in an attention module that generates samples based on the two ingredients; and (ii) node, edge and adjacency information are mutually dependent during the graph diffusion process. We evaluate our method on challenging benchmarks involving real-world and synthetic datasets in which edge features are crucial. Additionally, we introduce a new synthetic dataset that incorporates edge values. Furthermore, we propose a novel application that greatly benefits from the method due to its nature: the generation of traffic scenes represented as graphs. Our method outperforms other graph generation methods, demonstrating a significant advantage in edge-related measures.

1 Introduction

Generative modeling is a persistent challenge in numerous scientific and engineering fields, with broad practical use-cases. The primary goal is to understand the inherent distribution of a large database, enabling the generation of new samples. In many practical use-cases, using a graph representation is convenient for describing the samples, such as in molecule and protein design [Du et al., 2022], neural architecture search (NAS) [Oloulade et al., 2021], program synthesis [Gulwani et al., 2017], and more [Zhu et al., 2022].

The exploration of generative modeling is a longstanding endeavor, marked by the development of various methodologies throughout the years, including variational inference [Kingma and Welling, 2014], adversarial learning [Goodfellow et al., 2014], normalizing flows [Rezende and Mohamed, 2015], and diffusion models [Sohl-Dickstein et al., 2015]. Recently, generation of graph data has gained increased attention [Li et al., 2018, You et al., 2018]. In particular, the modeling of graph distributions through score-based approaches [Song and Ermon, 2019] stands out as a promising avenue that necessitates more comprehensive investigation.

Generally, a graph definition specifies several components that have a mutual interplay. One of which is the nodes which is a set of entities with possibly assigned attributes. The second is the adjacency information that specifies the nodes' connectivity, with potentially assigned features. As an example, one could use this structure to model a molecule. Here, nodes would represent atoms with atomic numbers as their attributes. In this context, the adjacency information could represent the intramolecular bonds and their types.

^{*}Ben-Gurion University, Beer Sheva, Israel

[†]Bosch Center of AI, Haifa, Israel

The involvement of several components in the graph whose attributes have a mutual interplay introduces a challenge of modeling the components altogether along with their relations. In order to address this challenge, Vignac et al. [2023] proposed a discrete diffusion approach for generating categorical node and edge attributes. However, extending it to sampling real-valued attributes remains non-trivial. Yet, while a discrete diffusion process fits well in certain cases, we advocate in this work the consideration of a more general problem with continuous score-based frameworks.

Recently, continuous score-based generative modeling of graphs was proposed in [Niu et al., 2020], focusing on estimating the adjacency matrix. To further sample node attributes, GDSS [Jo et al., 2022] solves separate stochastic differential equations (SDEs) for adjacency and nodes. In their formulation, the scores for different graph components are evaluated separately. Consequently, nodes are weakly affected by adjacent nodes during training and inference. Further, it exploits an attention mechanism using only node attributes and adjacency information to infer the graphs’ topology and their associated distributions. Additionally, existing methodologies [Fan et al., 2023] lack the capability to produce intricate edge features. In this work, we find that incremental adaptation to current approaches, with GDSS as a prime example, are insufficient and show that modeling diffusion processes with node and edge features is crucial.

Recent years have seen a surge in the utilization of score-based models in generative tasks [Song and Ermon, 2019, Jo et al., 2022]. While existing methods are performant under the absence of edge attributes generation, introducing such features causes them to fail immediately which hints towards the necessity of non-trivial modifications. In this study, we leverage the evident insight that edge attributes convey neighborhood information and provide instrumental data absent in the adjacency matrix that is crucial for generating edge attributes. We propose to encode graph distributions via a joint-SDE, describing the evolution of node and edge attributes. Importantly, our technique jointly solves for graph elements. Consequently, it benefits from the synergetic connections between nodes and edges. In comparison, GDSS [Jo et al., 2022] proposed a similar diffusion system for adjacency and nodes that is opt for a separated solution that may be sub-optimal in encoding certain graphs. We solve our joint-SDE by further strengthening the dependencies between nodes and edges. In practice, this is achieved by combining node, edge and adjacency information in an attention module, maximizing mutual interplay of the graph components. Overall, our approach is designed and implemented to maximally exploit the information encoded in the nodes and edges, and their interactions.

To evaluate our approach, we consider challenging benchmarks with dominant edge features. Specifically, we introduce a new synthetic dataset of grid mazes whose graphs are based on Markov decision processes. In this setting, edge attributes encode the probability of moving between grid cells. Further, we offer traffic scene generation on nuScenes [Caesar et al., 2020] as a new benchmark for evaluating edge-dominant generative graph methods. Finally, we define and estimate edge-related error metrics, allowing to quantitatively compare edge capabilities of generative models. **Our main contributions can be summarized as follows:**

- We introduce a novel inductive bias for score-based models in graph generation, leveraging a newly formulated Stochastic Differential Equation (SDE) approach that captures the interplay between edges and nodes. Additionally, our model incorporates an architectural bias to facilitate the propagation of edge information for better score estimation.
- We establish new links between graph generation and both MDPs and real-world traffic scenarios. We also advocate for a robust benchmark for edge-based graph generation assessments.
- We thoroughly evaluate our approach on diverse benchmark datasets and conduct ablation studies. Our results consistently demonstrate superior performance over baseline models, excelling across various standard evaluation protocols for graph generation tasks, particularly in edge metrics.

2 Related Work

Score-based generative models. Diffusion and score-based models represent generative models that sample new data by iteratively denoising a simple, pre-defined distribution [Sohl-Dickstein et al., 2015, Song and Ermon, 2019, Ho et al., 2020]. Song et al. [2021] showed that these methods can be described in a unified framework of stochastic differential equations (SDEs), thus we will use

the terms diffusion and score-based models interchangeably. The diffusion process consists of the forward pass, where noise is gradually added to the data until it converges to a normal Gaussian distribution, and the reverse pass, where a backward SDE is integrated using a denoising model. New samples are defined as the convergence points of the reverse pass. While several graph generative frameworks exist [Wu et al., 2020, Zhou et al., 2020], we focus on score-based approaches.

Discrete diffusion models. Haefeli et al. [2022] suggest discrete perturbations of the data distribution through a denoising diffusion kernel. Similarly, DiGress [Vignac et al., 2023] leveraged discrete diffusion methods [Austin et al., 2021] to produce discrete graphs containing categorical node and edge values. Recently, GraphARM [Kong et al., 2023] designed a node-absorbing autoregressive diffusion process for efficient and high-quality sampling. Chen et al. [2023] proposed a discrete diffusion process that utilize graph sparsity in the diffusion process to gain computational efficiency. While it is argued that discrete modeling of graphs may be beneficial, it is unclear how to sample real-valued attributes in existing frameworks. We insist that many real-world problems are naturally defined by continuous values, which requires the development of a general graph generative model as we propose.

Continuous diffusion models. Niu et al. [2020] introduced a permutation-invariant score-matching model based on graph neural networks (GNNs) for learning data distributions of adjacency matrices. To extract binary neighborhood information, the real-valued diffusion output is discretized via thresholding. Subsequently, GDSS [Jo et al., 2022] aims to improve the modelling of graph distributions via separate SDEs for node attributes and the adjacency matrix. Recently, SwinGNN [Yan et al., 2023] proposed a non-invariant approach for graph generation via diffusion, that can be made invariant by randomly permuting the sampled adjacency.

Following the success of graph score-based models, we are motivated to further extend this framework to include edge features. This is achieved by a careful inspection of GDSS, which results in the conclusion that separate scores for different components may lack context for the generation task. While trivial extensions exist, we find them to be unsatisfactory in solving even simple edge feature generation tasks, let alone challenging graph benchmarks. Instead, we address this problem by proposing a joint-SDE for all graph components, combined with a dedicated GNN architecture to exploit edge features. We show that our method greatly outperforms naive adaptations, demonstrating the necessity of each and every component we introduce as a whole.

Edge-based GNNs. We also mention a few works that consider edge-based GNNs for various tasks. R-GCN [Schlichtkrull et al., 2018] offered a decomposition where relational data is encoded more effectively. In Gong and Cheng [2019], the authors exploit edge features via doubly stochastic normalization. Similarly, Wang et al. [2021] extended popular GNN frameworks to handle edge features as well as node features. Motivated by these works, we explore graph generation by considering node and edge attributes.

3 Background

In what follows, we briefly discuss the essential components of score-based models on Euclidean domains \mathbb{R}^d . We refer the reader to [Song et al., 2021] for further details.

A *diffusion process* is defined by $\{x(t)\}_{t=0}^T$ with $t \in [0, T]$, where $x(0)$ is sampled from the data distribution $x(0) \sim p_0$; and $x(T) \sim p_T$, with p_T being a simple prior distribution such as a normal Gaussian. Diffusion processes are the solutions of SDEs of the form,

$$dx = f(x, t)dt + gdw, \quad (1)$$

where $f(\cdot, t) : \mathbb{R}^d \rightarrow \mathbb{R}^d$ is the drift coefficient, $g \in \mathbb{R}$ is the diffusion scalar, and w is a standard Wiener process. We adhere to standard notations and denote the probability density of $x(t)$ as $p_t(x)$, and the transition kernel from $x(s)$ to $x(t)$ for $s < t$ as $p_{st}(x(t) | x(s))$.

The process described in Eq. (1) is generative, as it allows for the generation of samples from $x(T) \sim p_T$, which can then be propagated backward through a reverse process. A well-known result by Anderson [1982] shows that the following reverse-time SDE is the reverse diffusion process,

$$dx = [f(x, t) - g^2 \nabla_x \log p_t(x)]d\bar{t} + g d\bar{w}, \quad (2)$$

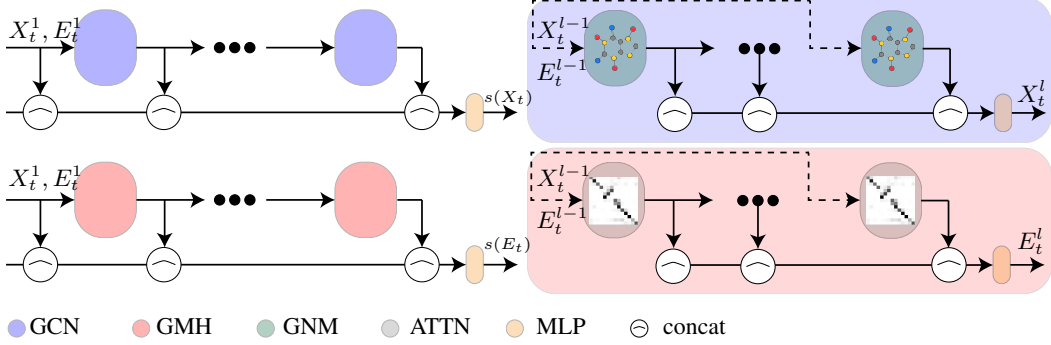


Figure 1: **The flow of our architecture.** On the left, the score modules high level architectures (Eq. 17 and Eq. 18). On the right (Blue), our GCN module (Eq. 12) constructed of GNM (Eq. 11) layers. On the right (Red), GMH module (Eq. 13) constructed of ATTN (Eq. 10) layers.

where \bar{w} is a reverse-time Wiener process, and $d\bar{t}$ denotes an infinitesimal negative timestep. Integration of Eq. (2) from time T to time 0 allows an effective sampling from p_0 .

Unfortunately, estimating the score, $\nabla_x \log p_t(x)$, is difficult for all timesteps except for $t = T$, that is defined as the prior distribution. Thus, score-based models [Song and Ermon, 2019] train an estimator $s_\theta(x, t)$ with the objective of

$$\min_{\theta} \mathbb{E}_t \{ \mathbb{E}_{x_0, x_t} [|s_\theta(x_t, t) - \nabla_{x_t} \log p_{0t}(x_t | x_0)|_2^2] \}. \quad (3)$$

4 Method

Our method to generative modeling of graphs is based on two novelties. First, we propose a joint score-based model of node and edge attributes (Sec. 4.1), where the resulting sample’s score is evaluated for all graph components jointly. Second, we combine node, edge and adjacency information in the attention building block (Sec. 4.2). With these two key ingredients, we achieve a modeling of graphs as a whole.

4.1 A Joint SDE Model

The main goal of our model is to represent the data distribution of graphs, denoted p_0 . A graph with n nodes is a 2-tuple $G = (X, E)$, where $X \in \mathbb{R}^{n \times u}$ are the node attributes and $E \in \mathbb{R}^{n \times n \times v}$ is the edge attributes tensor. Importantly, the adjacency matrix $A \in \{0, 1\}^{n \times n}$ can be recovered from E by a simple mask such as

$$A := \sigma(\max_k |E_{ijk}|), \quad (4)$$

where $\sigma = 0$ if $\sigma(x) < \epsilon$ and else $\sigma = 1$. We chose $\epsilon = 0.01$ for all datasets. Thus, encoding $G = (X, E)$ is sufficient to fully capture the underlying structure of the graph. We would like to generate new graphs $G \sim p_0$, which we achieve by defining a diffusion process from p_0 to p_T (and back), as we describe below.

We follow the general outline in Sec. 3. A diffusion process on $\{G_t = (X_t, E_t)\}_{t=0}^T$ is given by the SDE,

$$dG_t = f(G_t, t)dt + gdw, \quad (5)$$

where f is the drift transformation on a set of graphs \mathcal{G} , i.e., $f(\cdot, t) : \mathcal{G} \rightarrow \mathcal{G}$. The corresponding reverse-time SDE reads

$$dG_t = [f(G_t, t) - g^2 \nabla_{G_t} \log p_t(G_t)]d\bar{t} + gdw, \quad (6)$$

where in Eqs. (5) and (6), we abuse the notation that appeared in Eqs. (1) and (2), while keeping the equivalent meaning for g , w , \bar{w} and $d\bar{t}$ on graphs. Analogously to Eq. (3), the score $\nabla_{G_t} \log p_t(G_t)$ is estimated using a graph neural network whose objective is

$$\min_{\theta} \mathbb{E}_t \{ \mathbb{E}_{*} [|s_\theta(G_t, t) - \nabla_{G_t} \log p_{0t}(G_t | G_0)|_2^2] \}, \quad (7)$$

where $G_0 \sim p_0$, $G_t \sim p_{0t}(G_t | G_0)$, and the expectation \mathbb{E}_* is taken over G_0 and $G_t | G_0$.

A similar diffusion process as in Eq. (5) was considered in GDSS. However, instead of solving the joint SDE, they use separate processes for the nodes and adjacency. Consequently, nodes and their neighbors affect each other only through the score function. On the other hand, we aim to solve it jointly for node and edge attributes, allowing them to interact during the diffusion process through the score calculation, as well as the drift function. This modification will also be emphasized below where we elaborate on our graph neural network whose illustration is given in Fig. 1.

4.2 Node and Edge-Dependent GNN

Similar to existing generative works [Niu et al., 2020, Jo et al., 2022], we adopt the framework of graph neural networks [Wu et al., 2020], and specifically, the graph multi-head attention module [Baek et al., 2021]. A fundamental element within our strategy is the Graph Neural Module (GNM), where nodes, edges, and adjacency exchange information. Notably, the GNM is a basic building block in our architecture that enables interaction between the graph elements whose values determine graph generation, closely following the general idea of our score-based model in Eq. (5).

Graph neural module. Given an intermediate estimation of node and edge attributes, denoted by X_t and E_t , respectively, the GNM module is defined via

$$\text{GNM}(X_t, E_t) := \bar{A}_t X_t W_X + \tanh(B[\bar{A}_t \odot E_t W_E]), \quad (8)$$

where \odot is the element-wise product, W_X, W_E are neural network weights. $B[\cdot]$ sums the values of each node incoming edges feature-wise. Inspired by Kipf and Welling [2017], we construct the matrix \bar{A}_t by scaling the adjacency A_t with the degree matrix D_t , i.e.,

$$\bar{A}_t = D_t^{-\frac{1}{2}} \odot A_t \odot D_t^{-\frac{1}{2}}, \quad (9)$$

where D_t is a diagonal matrix, encoding the number of edges per node. Finally, A_t is extracted via Eq. (4).

Attention module. We also employ a commonly-used partial attention module, ATTN Baek et al. [2021]. Formally,

$$\text{ATTN}(X_t, E_t) := \text{avg} \left(Q_t K_t^T / \sqrt{d_t} \right), \quad (10)$$

with $Q_t := \text{GNM}_Q(X_t, E_t)$ and $K_t := \text{GNM}_K(X_t, E_t)$, $\text{avg}(\cdot)$ computes the mean over the axis of the different attention channels, and d_t is the attention dimension.

Our graph neural network. We utilize the GNM and ATTN modules to construct our full graph neural network to compute the score $s_\theta(G_t, t)$. To simplify notation, we define $H(\{h_j\}, J, M)$ as the module that takes a collection of vectors $\{h_j\}$ with J elements, concatenates them, and feeds the result through a multilayer perceptron (MLP) M :

$$H(\{h_j\}, J, M) := M \left(\text{concat} [h_j]_{j=1}^J \right). \quad (11)$$

Then, we define two components that will be used to generate the node and edge attributes. The graph convolutional network (GCN) is given by

$$\text{GCN}(X_t, E_t) = H(\{\text{GNM}(X_t, E_t)_j\}, J, M_\varphi), \quad (12)$$

and the graph multi-head attention (GMH) is defined by

$$\text{GMH}(X_t, E_t) := H(\{\text{ATTN}(X_t, E_t)_j\}, J, M_\phi). \quad (13)$$

Finally, we define the score $s_\theta(G_t, t)$ by

$$s_\theta(G_t, t) := (s_\theta^X(X_t, E_t, t), s_\theta^E(X_t, E_t, t)). \quad (14)$$

To estimate the aforementioned score function, we use feed-forward neural networks F_X and F_E as follows. Given initial node and edge attributes, denoted as $X_t^1 = X_t$ and $E_t^1 = E_t$ respectively, The model sequentially alters its inputs as they pass through the layers by

$$X_t^l := F_X^l(X_t^{l-1}, E_t^{l-1}) \equiv \text{GCN}(X_t^{l-1}, E_t^{l-1}), \quad (15)$$

$$E_t^l := F_E^l(X_t^{l-1}, E_t^{l-1}) \equiv \text{GMH}(X_t^{l-1}, E_t^{l-1}). \quad (16)$$

Here, X_t^l, E_t^l denote the node and edge attributes representing the output of the l -th layer, $l \in [1, L]$. Our computation is completed by

$$s_{\theta}^X(X_t, E_t, t) = H(\{X_t^l\}, L, M_{\theta_X}), \quad (17)$$

$$s_{\theta}^E(X_t, E_t, t) = H(\{E_t^l\}, L, M_{\theta_E}). \quad (18)$$

Overall, our modification in Eq. (8) allows for a proper digestion of the edge information by the score network and its propagation through the entire score model. We consider this formulation to be crucial for estimating the score, as demonstrated in Section 5.5.

Complexity Analysis The time-complexity is governed by the attention mechanism. Specifically, both GMH and GCN modules introduce a $\mathcal{O}(n^2)$ component for time that scales linearly with the number of attention heads and the input/output feature dimensionalities. Additionally, storage for edge features requires $\mathcal{O}(n^2v)$, with v being the number of features. Thus, our approach is similar in time and memory complexity to other SOTA models such as DiGress [Vignac et al., 2023] and GDSS [Jo et al., 2022].

5 Experiments

We tested our method both qualitatively and quantitatively on multiple diverse benchmarks of real-world and synthetic datasets. The objectives of this study are:

- We ablate our model on several benchmarks to analyze the contribution of every component to its performance (Sec. 5.4). This is concluded with an empirical evaluation of the score estimation quality (Sec. 5.5).
- As our primary focus is to enable the generation of edge features, we show in Sec. 5.1 that incremental modifications of GDSS are less effective, highlighting the non-trivial importance of our approach.
- We introduce a new challenging synthetic dataset of Markov decision processes (Sec. 5.2). Further, we present a new use case; a real-world traffic generation task (Sec. 5.3). To the best of our knowledge, we are the first to tackle this task via graph generation.

5.1 Synthetic Dataset Ablation Experiment

We conduct an in-depth study to analyze the performance gain contributed by incorporating our different components. Additionally, we aim to show that current methods, even with incremental adaptations to edge feature generation, are ineffective for the edge generation task.

Dataset. We utilize a synthetic dataset of 1000 complete graphs, with only edge attributes. The nodes do not contain any information. Let E be the set of edges in a sampled graph. Each $e \in E$ belongs to \mathbb{R}^2 and the two features in e are homogeneous and sampled randomly from *only one* of the Gaussian clusters depicted in Fig. 2a.

Baseline and variates. To create a solid baseline, we adapt GDSS to handle multiple edge features, and we name it *GDSS-E*. A detailed description can be found in App. A.2.2. *GDSS-E* can be seen as a vanilla model without our novel contributions. Then, to ablate our two model components, we separate each of them and add them separately to the vanilla baseline model. We denote the baseline with our joint SDE model (Eq. 7) as *Joint-SDE-Model*, and the baseline with our GNM model (Eq. 8) as *GNM-Based-Model*. Finally, our approach is based on *GDSS-E* and comprises of both of the above components.

Evaluation. Fig. 2 contains scatter plots of the edge distributions. For this visualization, we generate 500 complete graphs with 5000 edges in total. The desired result would be a generation of edge features similar to the ground-truth in Fig. 2a. We qualitatively compare the different variant baselines in Fig. 2. A good model should generate the same visual clustering as the ground-truth. Further, to evaluate the edge features quantitatively, we consider the homogeneity of edges. For every graph, we check the percentage of edges that are homogeneous, i.e., edges whose both nodes

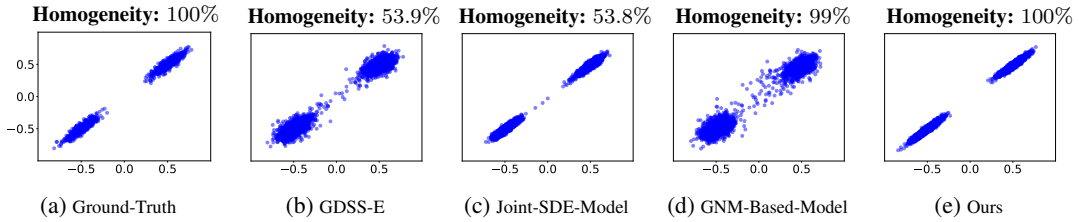


Figure 2: Our ablation study shows that GDSS-E and the other variants yield inferior distributions compared to our approach concerning the ground-truth data distribution estimation.

belong to only one of the clusters. Then, we compute the average percentage of this test for the 5000 generated samples per method. We detail the homogeneity score above each plot, where good models should yield 100%, as the ground-truth.

Results. Fig. 2b shows that GDSS-E roughly approximates the distribution. However, the two clusters appear blurred, making it difficult to differentiate between them. In addition, it fails to learn the homogeneity characteristics of the data. The Joint-SDE-Model (Fig. 2c) presents improved results by estimating denser Gaussian clusters. Alas, it fails to yield a fine grained generation as some samples are outside the original distribution (e.g., the points around 0). Further, this model also fails in the homogeneity task. The GNM-Based-Model (Fig. 2d) generates blurred and non-separated clusters. Nevertheless, it successfully models homogeneous edge features, achieving a 99% homogeneity score. Finally, our approach (Fig. 2e) demonstrates a similar distribution to the ground-truth in terms of separation and clusters’ structure, as well as a perfect homogeneity score.

These results shed light on the importance of our components. On the one hand, our joint-SDE process accurately models the underlying distribution, but it struggles with preserving homogeneity, i.e., with interactions between features within an edge. On the other hand, the GNM-based model succeeds in maintaining homogeneous aspects, but it is challenged by the data distribution. We conclude that our new components are important: 1) the joint-SDE process is crucial in modeling inter-edge interactions; and 2) the GNM module is instrumental in capturing intra-edge relationships.

5.2 Generative MDPs

Reinforcement Learning (RL) environments typically consist of multiple states and the probabilities to move from one state to another. These environments are often formalized as Markov Decision processes (MDPs) which can be viewed as directed graphs, where nodes represent states and edge attributes represent the transition probabilities. We strive to explore the connection between generative modeling of graphs and MDPs. Indeed, access to many diverse RL environments is often limited in practice, we aim to extend and diversify available environments.

In this context, we introduce a new synthetic MDP dataset of grid mazes. Each grid has 5×5 cells, including a start cell and a goal cell. Some of the cells represent obstacles. Generally, agents take one action per cell {up, left, down, right}. The maze is encoded via a graph whose nodes are the cells, and edges are the optional transitions. The attributes are the probabilities of moving from the current cell to one of its adjacent cells. Here, we consider two settings of using this data: (1) a deterministic grid maze, where edge features are binary in $\{0, 1\}$; and (2) a non-deterministic grid maze, where edge attributes are probabilities in $[0, 1]$, and the sum of all features per cell is one. Further details on these datasets and their MDP graphs is provided in App. A.1.1.

A unique characteristic of our MDP graphs is their multiple attributes per edge. To the best of our knowledge, this scenario is barely studied in existing generative works. In particular, prior works are designed to construct only a single edge value. Nevertheless, to compare our approach against strong baselines, we consider the state-of-the-art GDSS, and we modify it to GDSS-E as discussed in Sec. 5.1.

To quantitatively evaluate the graphs, we utilize common metrics such as the degree (deg) and cluster (cl). We do not use the orbit metric since the grid maze MDPs are directed cyclic graphs. Further, we introduce five new dataset-specific and edge-based metrics that measure the quality of generated graphs and edge features. Valid solution (VS) tests if the grid is valid, i.e., it has start and finish cells with a viable route between them. Blocks (B) measures the distance between the average number

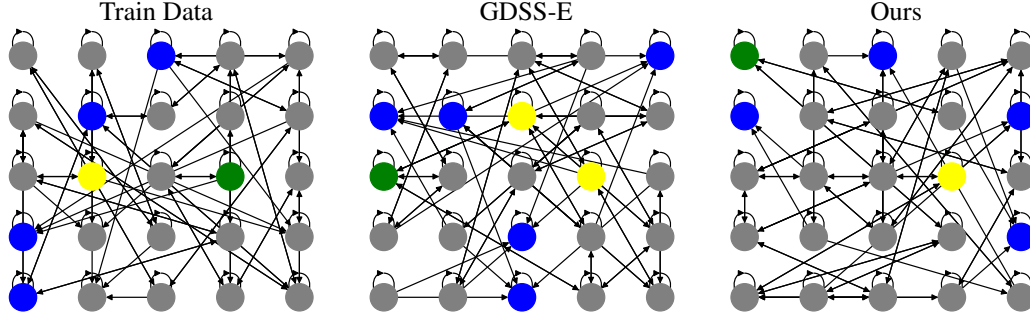


Figure 3: A qualitative comparison between the original data (left), GDSS-E (middle), and our method (right) on the deterministic MDP grid maze dataset. Obstacles are colored in blue, and start and finish nodes in yellow and green, respectively. Our graphs consistently have four obstacles, one start node, and one finish node, as required.

of obstacles in the grid, where in our dataset the ground-truth value is four. Start and finish (SF) calculates the distance between the average number of start and finish cells, which are always two in our grids. Empty (E) computes the distance between the average number of regular cells. Finally, MDP validity (MV) estimates the percentage of valid edge features in the generated graphs. Features are valid if the sum of the outgoing edges of a node is equal to 1. The results of our evaluation on grid maze MDPs are shown in Tab. 1.

The deterministic setting. Our approach better captures the graph statistics measured by the degree (deg) and cluster (cl) metrics, showing a significant gap with respect to GDSS-E. Further, our graphs’ edge-based metric, MV, is twice the baseline result, i.e., **68%** vs. 34%. These results emphasize our model’s ability to capture edge attribute complexities. Finally, our model achieves strong results in the metrics that estimate node generation compared to GDSS-E.

We also present a qualitative comparison of the real training data, the generated graphs obtained with GDSS-E, and our approach. Fig. 3 shows a sample from the training data (left), a graph generated with GDSS-E (middle), and our generated graph (right). The colored nodes are obstacles (blue) and start and finish cells (yellow and green, respectively). Our method yields a valid graph, respecting the correct number of obstacles and start and finish points. In contrast, GDSS-E has two starting points and five obstacle nodes.

The non-deterministic case. In this setting, where edge features are real-valued, edge features are valid if its MV measure is $\epsilon = 0.001$ close to one. Further, the edge values follow a specific pre-defined distribution, and thus, in addition to MV, we also measure the MDP distribution validity (MDV).

Namely, the percentage of edges that follow the distribution above. Notably, the measures in Tab. 1 our model obtains are ≈ 6 times better than the baseline on the edge-related metrics, MV and MDV. These results affirm our framework’s ability to effectively capture and generate diverse and complex multiple-edge attributes.

Table 1: Quantitative graph generation metrics on deterministic and non-deterministic grid mazes.

Method	deterministic							non-deterministic							
	deg↓	cl↓	MV↑	VS↑	B↓	SF↓	E↓	deg↓	cl↓	MV↑	MDV↑	VS↑	B↓	SF↓	E↓
GDSS-E	0.73	0.06	34%	9%	0.96	1.28	2.23	0.40	0.02	6%	1%	26%	0.39	0.83	0.4
Ours	0.17	0.006	68%	34%	0.1	0.58	0.48	0.31	0.013	38%	6%	33%	0.02	0.88	0.8

5.3 nuScenes: traffic scene generation

Learning traffic scenes can hugely contribute to autonomous driving tasks. To the best of our knowledge, we are the first to suggest a generation of traffic scenes as graphs. We leverage the idea that a scene with elements such as cars, tracks, traffic lights, lanes, and more can be represented as a graph. In this graph, each node is an agent containing the trajectory across time, and each directed edge represents the effect of one agent on another. Edge features such as Euclidean distances and angles are optional.

In what follows, we use nuScenes [Caesar et al., 2020], a public dataset that is broadly used for trajectory prediction [Liu et al., 2021]. Primarily, the challenge is to predict a future trajectory from the history traces of a road participant. We transform each scene into a vector-graph representation, similar to VectorNet [Gao et al., 2020]. The latter work was the first to utilize a graph representation of the scenes, where nodes represent agents and map elements, which are later processed via GNNs to predict the target. Refer to App. A.1.2 for more details about the dataset.

We compute the standard graph statistical metrics for directed graphs and common evaluation protocols for traffic generation [Tan et al., 2023, Feng et al., 2023]: vehicles MMD (V), object MMD (O), lanes MMD (L), collusion rate (CR), and lane alignment (LA). Refer to App. A.1.1 for further details on the graph representation, training, and evaluation protocols.

We display in Tab. 2 our results in comparison to the GDSS-E baseline. Generally, our model outperforms the baseline in most general and traffic-specific metrics. In particular, we observe that our model captures the location statistics of the vehicles (V) and the lanes (L) with a significant gap of ≈ 10 times better than the baseline.

Table 2: Quantitative metrics on nuScenes.

Method	deg↓	cl↓	V↓	O↓	L↓	CR↓	LA↓
GDSS-E	1.05	0.03	3.9	0.66	0.96	0.5%	208
Our	0.77	$6e^{-7}$	0.36	0.8	0.08	0.3%	194

5.4 Ablation Study

Edge-based graphs benchmark ablation. We extend our ablation study in Sec. 5.1 and consider the four model variants. We perform our quantitative ablation over deterministic MDP (MDP-D), non-deterministic MDP (MDP-ND), and nuScenes.

We report the results of the standard error metrics, deg, cl, and MV or LA in Tab. 3. We omit some metrics due to space constraints. However, the trend is similar in those metrics as well. Our results indicate that the proposed model obtains the best results across all datasets and metrics, except for LA in nuScenes. Further, we find that only incorporating edge-based GNM, leads to inconsistent behavior. However, jointly modeling node and edge attributes attains a notable gain in error metrics. Finally, using both components leads to the best results.

Table 3: Ablation study of the four variants of our model.

Method	MDP-D			MDP-ND			nuScense		
	deg↓	cl↓	MV↑	deg↓	cl↓	MV↑	deg↓	cl↓	LA ↓
GDSS-E	0.73	0.06	34%	0.40	0.02	26%	1.05	0.03	208
Joint-SDE-Model	0.71	0.05	57%	1.67	0.54	2%	1.4	0.02	243
GNM-Based-Model	0.23	0.02	55%	0.35	0.07	33%	0.99	$1e^{-5}$	179
Ours	0.17	0.006	68%	0.31	0.013	33%	0.77	$6e^{-7}$	194

General graphs benchmark ablation. Although our study focuses on edge-dominant graph benchmarks, we apply our method to general graph generation tasks and extend the ablation study to show our model robustness to different diverse datasets. To leverage edge attribute abilities of our model, we augment every graph with edge attributes per edge. Specifically, we compute the n -th power of the adjacency matrix, and then, for each edge e_{ab} between nodes a and b , we assign the corresponding value encoded in the power matrix. The edge features contain the number of paths between a and b with n steps, where we set $n = 2$.

In Tab. 4 we report the results on the Planar and SBM datasets. We observe a similar trend as in the previous ablation, and our method outperforms the other variants. In addition to the ablation study, we compare general graph benchmarks with augmented features at App. B.1. We show our model can learn the graph distribution better with edge features, and we achieve competitive results concerning solid baselines.

Table 4: Ablation study of the four variants of our model.

Method	Planar			SBM		
	deg↓	cl↓	orb↓	deg↓	cl↓	orb↓
GDSS-E	0.945	0.96	0.66	0.74	1.57	0.25
Joint-SDE-Model	1.02	0.94	0.26	0.2	1.04	0.05
GNM-Based-Model	0.038	0.95	0.22	0.34	0.7	0.05
Ours	0.025	0.38	0.23	0.46	0.63	0.04

5.5 Comparison of Score Losses

In this experiment, we compare the behavior of graph generation models in terms of the node and edge score losses on the train and test sets. We report these losses throughout training on the nuScenes dataset in Fig. 4.

The left column corresponds to the train set, and the right to the test set. The top row shows the node losses, whereas the bottom row shows the edge losses. We use blue and orange for the loss measures of our method and GDSS-E, respectively. While the node score losses are comparable for both models, our method yields significantly better edge losses.

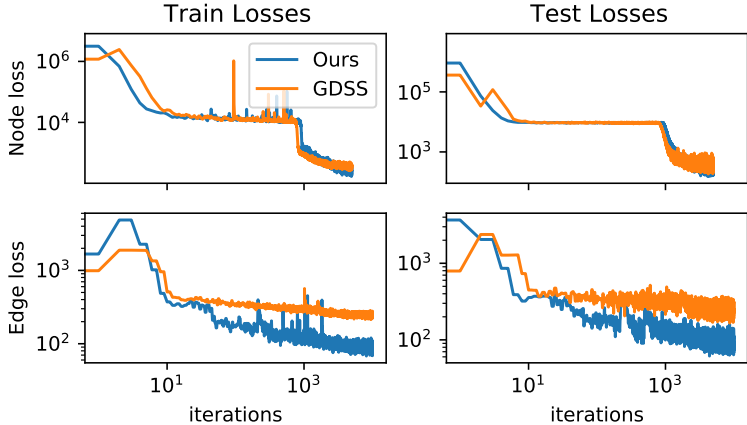


Figure 4: We plot the node and edge scores of GDSS-E and our model on the train (left) and test (right) sets.

6 Conclusion

While graph generation models must consider all graph elements and their interactions, existing works focus only on adjacency and node attributes. Further, score-based methods utilize a separate diffusion process per graph element, which limits the interaction between the sampled components. This work suggests a joint score-based model for node and edge features. Our framework maximizes learning from graph elements by combining node and edge attributes in the attention-building block module. Moreover, node, edge, and adjacency information are mutually dependent on construction in the diffusion process.

We extensively evaluate our approach on multiple synthetic and real-world benchmark datasets compared to recent strong baselines. Further, we introduced a new synthetic dataset for benchmarking edge-based approaches. Our results show that exploiting edge information is instrumental to general and edge-related metrics performance.

In the future, we would like to incorporate certain inductive biases into the generation pipeline. For instance, MDPs and nuScenes are challenging benchmarks that may enormously benefit from such an approach. Moreover, generating new samples with diffusion frameworks is costly, and we want to improve this aspect. Increasing the expressivity of GNN is an exciting research avenue, potentially letting go of the permutation invariance property.

References

- Brian DO Anderson. Reverse-time diffusion equation models. *Stochastic Processes and their Applications*, 12(3):313–326, 1982.
- Jacob Austin, Daniel D Johnson, Jonathan Ho, Daniel Tarlow, and Rianne Van Den Berg. Structured denoising diffusion models in discrete state-spaces. *Advances in Neural Information Processing Systems*, 34:17981–17993, 2021.
- Jinheon Baek, Minki Kang, and Sung Ju Hwang. Accurate learning of graph representations with graph multiset pooling. In *9th International Conference on Learning Representations, ICLR*, 2021.
- Holger Caesar, Varun Bankiti, Alex H Lang, Sourabh Vora, Venice Erin Liong, Qiang Xu, Anush Krishnan, Yu Pan, Giancarlo Baldan, and Oscar Beijbom. nuScenes: A multimodal dataset for autonomous driving. In *Proceedings of the IEEE/CVF conference on computer vision and pattern recognition*, pages 11621–11631, 2020.
- Xiaohui Chen, Jiaxing He, Xu Han, and Li-Ping Liu. Efficient and degree-guided graph generation via discrete diffusion modeling. *arXiv preprint arXiv:2305.04111*, 2023.
- Nachiket Deo, Eric Wolff, and Oscar Beijbom. Multimodal trajectory prediction conditioned on lane-graph traversals. In Aleksandra Faust, David Hsu, and Gerhard Neumann, editors, *Proceedings of the 5th Conference on Robot Learning*, volume 164 of *Proceedings of Machine Learning Research*, pages 203–212. PMLR, 08–11 Nov 2022. URL <https://proceedings.mlr.press/v164/deo22a.html>.
- Yuanqi Du, Tianfan Fu, Jimeng Sun, and Shengchao Liu. Molgensurvey: A systematic survey in machine learning models for molecule design. *arXiv preprint arXiv:2203.14500*, 2022.
- Wenqi Fan, Chengyi Liu, Yunqing Liu, Jiatong Li, Hang Li, Hui Liu, Jiliang Tang, and Qing Li. Generative diffusion models on graphs: Methods and applications. *arXiv preprint arXiv:2302.02591*, 2023.
- Lan Feng, Quanyi Li, Zhenghao Peng, Shuhan Tan, and Bolei Zhou. Trafficgen: Learning to generate diverse and realistic traffic scenarios. In *2023 IEEE International Conference on Robotics and Automation (ICRA)*, pages 3567–3575. IEEE, 2023.
- Jiyang Gao, Chen Sun, Hang Zhao, Yi Shen, Dragomir Anguelov, Congcong Li, and Cordelia Schmid. Vectormet: Encoding hd maps and agent dynamics from vectorized representation. In *Proceedings of the IEEE/CVF Conference on Computer Vision and Pattern Recognition (CVPR)*, June 2020.
- Liyu Gong and Qiang Cheng. Exploiting edge features for graph neural networks. In *Proceedings of the IEEE/CVF conference on computer vision and pattern recognition*, pages 9211–9219, 2019.
- Ian Goodfellow, Jean Pouget-Abadie, Mehdi Mirza, Bing Xu, David Warde-Farley, Sherjil Ozair, Aaron Courville, and Yoshua Bengio. Generative adversarial networks. *Advances in neural information processing systems*, 27, 2014.
- Sumit Gulwani, Oleksandr Polozov, Rishabh Singh, et al. Program synthesis. *Foundations and Trends® in Programming Languages*, 4(1-2):1–119, 2017.
- Kilian Konstantin Haefeli, Karolis Martinkus, Nathanaël Perraudin, and Roger Wattenhofer. Diffusion models for graphs benefit from discrete state spaces. *arXiv preprint arXiv:2210.01549*, 2022.
- Jonathan Ho, Ajay Jain, and Pieter Abbeel. Denoising diffusion probabilistic models. *Advances in neural information processing systems*, 33:6840–6851, 2020.
- Jaehyeong Jo, Seul Lee, and Sung Ju Hwang. Score-based generative modeling of graphs via the system of stochastic differential equations. In *International Conference on Machine Learning*, pages 10362–10383. PMLR, 2022.
- ByeoungDo Kim, Seong Hyeon Park, Seokhwan Lee, Elbek Khoshimjonov, Dongsuk Kum, Junsoo Kim, Jeong Soo Kim, and Jun Won Choi. Lapred: Lane-aware prediction of multi-modal future trajectories of dynamic agents. In *Proceedings of the IEEE/CVF Conference on Computer Vision and Pattern Recognition*, pages 14636–14645, 2021.
- Diederik P Kingma and Jimmy Ba. Adam: A method for stochastic optimization. *arXiv preprint arXiv:1412.6980*, 2014.
- Diederik P. Kingma and Max Welling. Auto-encoding variational bayes. In *2nd International Conference on Learning Representations, ICLR*, 2014.

- Thomas N. Kipf and Max Welling. Semi-supervised classification with graph convolutional networks. In *5th International Conference on Learning Representations, ICLR*, 2017.
- Lingkai Kong, Jiaming Cui, Haotian Sun, Yuchen Zhuang, B. Aditya Prakash, and Chao Zhang. Autoregressive diffusion model for graph generation. In *International Conference on Machine Learning, ICML*, volume 202 of *Proceedings of Machine Learning Research*, pages 17391–17408. PMLR, 2023.
- Yujia Li, Oriol Vinyals, Chris Dyer, Razvan Pascanu, and Peter Battaglia. Learning deep generative models of graphs. *arXiv preprint arXiv:1803.03324*, 2018.
- Jianbang Liu, Xinyu Mao, Yuqi Fang, Delong Zhu, and Max Q-H Meng. A survey on deep-learning approaches for vehicle trajectory prediction in autonomous driving. In *2021 IEEE International Conference on Robotics and Biomimetics (ROBIO)*, pages 978–985. IEEE, 2021.
- Mengmeng Liu, Hao Cheng, Lin Chen, Hellward Broszio, Jiangtao Li, Runjiang Zhao, Monika Sester, and Michael Ying Yang. Laformer: Trajectory prediction for autonomous driving with lane-aware scene constraints. *arXiv preprint arXiv:2302.13933*, 2023.
- Karolis Martinkus, Andreas Loukas, Nathanaël Perraudin, and Roger Wattenhofer. Spectre: Spectral conditioning helps to overcome the expressivity limits of one-shot graph generators. In *International Conference on Machine Learning*, pages 15159–15179. PMLR, 2022.
- Chenhao Niu, Yang Song, Jiaming Song, Shengjia Zhao, Aditya Grover, and Stefano Ermon. Permutation invariant graph generation via score-based generative modeling. In *International Conference on Artificial Intelligence and Statistics*, pages 4474–4484. PMLR, 2020.
- Babatounde Moctard Oloulade, Jianliang Gao, Jiamin Chen, Tengfei Lyu, and Raaed Al-Sabri. Graph neural architecture search: A survey. *Tsinghua Science and Technology*, 27(4):692–708, 2021.
- Danilo Rezende and Shakir Mohamed. Variational inference with normalizing flows. In *International conference on machine learning*, pages 1530–1538. PMLR, 2015.
- Michael Schlichtkrull, Thomas N Kipf, Peter Bloem, Rianne Van Den Berg, Ivan Titov, and Max Welling. Modeling relational data with graph convolutional networks. In *The Semantic Web: 15th International Conference, ESWC*, pages 593–607. Springer, 2018.
- Ida Schomburg, Antje Chang, Christian Ebeling, Marion Gremse, Christian Heldt, Gregor Huhn, and Dietmar Schomburg. Brenda, the enzyme database: updates and major new developments. *Nucleic acids research*, 32 (suppl_1):D431–D433, 2004.
- Prithviraj Sen, Galileo Namata, Mustafa Bilgic, Lise Getoor, Brian Galligher, and Tina Eliassi-Rad. Collective classification in network data. *AI magazine*, 29(3):93–93, 2008.
- Martin Simonovsky and Nikos Komodakis. Graphvae: Towards generation of small graphs using variational autoencoders. In *Artificial Neural Networks and Machine Learning–ICANN 2018: 27th International Conference on Artificial Neural Networks, Rhodes, Greece, October 4–7, 2018, Proceedings, Part I 27*, pages 412–422. Springer, 2018.
- Jascha Sohl-Dickstein, Eric Weiss, Niru Maheswaranathan, and Surya Ganguli. Deep unsupervised learning using nonequilibrium thermodynamics. In *International conference on machine learning*, pages 2256–2265. PMLR, 2015.
- Yang Song and Stefano Ermon. Generative modeling by estimating gradients of the data distribution. *Advances in neural information processing systems*, 32, 2019.
- Yang Song, Jascha Sohl-Dickstein, Diederik P. Kingma, Abhishek Kumar, Stefano Ermon, and Ben Poole. Score-based generative modeling through stochastic differential equations. In *9th International Conference on Learning Representations, ICLR*, 2021.
- Shuhan Tan, Kelvin Wong, Shenlong Wang, Sivabalan Manivasagam, Mengye Ren, and Raquel Urtasun. Scenegen: Learning to generate realistic traffic scenes. In *Proceedings of the IEEE/CVF Conference on Computer Vision and Pattern Recognition*, pages 892–901, 2021.
- Shuhan Tan, Boris Ivanovic, Xinshuo Weng, Marco Pavone, and Philipp Kraehenbuehl. Language conditioned traffic generation. *arXiv preprint arXiv:2307.07947*, 2023.
- Clément Vignac, Igor Krawczuk, Antoine Siraudin, Bohan Wang, Volkan Cevher, and Pascal Frossard. Digress: Discrete denoising diffusion for graph generation. In *The Eleventh International Conference on Learning Representations, ICLR*, 2023.

- Ziming Wang, Jun Chen, and Haopeng Chen. Egat: Edge-featured graph attention network. In *Artificial Neural Networks and Machine Learning–ICANN*, pages 253–264. Springer, 2021.
- Zhenqin Wu, Bharath Ramsundar, Evan N Feinberg, Joseph Gomes, Caleb Geniesse, Aneesh S Pappu, Karl Leswing, and Vijay Pande. Moleculenet: a benchmark for molecular machine learning. *Chemical science*, 9(2):513–530, 2018.
- Zonghan Wu, Shirui Pan, Fengwen Chen, Guodong Long, Chengqi Zhang, and S Yu Philip. A comprehensive survey on graph neural networks. *IEEE transactions on neural networks and learning systems*, 32(1):4–24, 2020.
- Qi Yan, Zhengyang Liang, Yang Song, Renjie Liao, and Lele Wang. Swingnn: Rethinking permutation invariance in diffusion models for graph generation. *arXiv preprint arXiv:2307.01646*, 2023.
- Jiaxuan You, Rex Ying, Xiang Ren, William Hamilton, and Jure Leskovec. Graphrnn: Generating realistic graphs with deep auto-regressive models. In *International conference on machine learning*, pages 5708–5717. PMLR, 2018.
- Jie Zhou, Ganqu Cui, Shengding Hu, Zhengyan Zhang, Cheng Yang, Zhiyuan Liu, Lifeng Wang, Changcheng Li, and Maosong Sun. Graph neural networks: A review of methods and applications. *AI open*, 1:57–81, 2020.
- Yanqiao Zhu, Yuanqi Du, Yinkai Wang, Yichen Xu, Jieyu Zhang, Qiang Liu, and Shu Wu. A survey on deep graph generation: Methods and applications. In *Learning on Graphs Conference*, pages 47–1. PMLR, 2022.

A Additional Details

A.1 Datasets

A.1.1 MDP Grid Maze - Datasets

Motivation. We propose an innovative link between graph generation techniques and Markov Decision Processes (MDPs). Generating various environments for agents is crucial in Reinforcement Learning (RL) for effective task learning. However, there are instances where access to diverse environments is limited. Environments can be formalized as MDPs, and MDPs can be represented as directed graphs. Thus, we are motivated to create a new dataset whose graphs contain node and edge attributes and are directed graphs. Such data will diversify the common standard benchmarks today that include undirected graphs and contain only one type of feature, either for nodes or edges.

Dataset Description. We create two variants of the MDP grid maze dataset: deterministic and non-deterministic. In both settings, the grid is the same. However, the probability of an action is different. In both datasets, the node $u \in \mathbb{R}^{25 \times 3}$ contains in its first coordinate the cell value: -1 for the block cell, 0 for the neutral cell, 1 for the starting cell and finally, $a \sim [0.5, 1]$ for the finish point. Blocks and the finish line could also be considered as prizes or punishments; however, in our graph representation, blocks are cells that are out of reach. An outgoing edge $e_{uv} \in \mathbb{R}^4$ between node u and v equals to $p(v|u, a)$, which is the probability of getting to node v from u given an action a . There are four actions: $\mathcal{A} = \{left, up, right, down\}$. Note, a valid MDP is where for all state $u \in \mathcal{S}$, $v \in \mathcal{S}$ and actions $a \in \mathcal{A}$ the sum of all actions:

$$\sum_{\substack{a \in \mathcal{A} \\ v \in \mathcal{S}}} p(v|u, a) = 1. \tag{19}$$

An equivalent constraint is that all node's outgoing edges u will sum to 1. Finally, the graph's connectivity is decided by the following rules: (1) Moving toward a block is impossible. Therefore, there is an edge toward blocks with probability zero. (2) Block cells have no outgoing edges. (3) The grid perimeter is closed; thus, moving outside the grid is impossible. (4) Finally, all other moves are legal.

In Fig.5, we present the grid (left) and its graph representation(center) without edge values for simplicity (we later present a more straightforward graph with edge values). In addition, we show a permuted representation of the same graph (right). There are $25!$ ways to represent the same graph. Although it looks completely different, both representations represent the same grid maze. The yellow cell is the starting point, the green cell is the ending point, dark blue is the block cells, and the gray cells are neutral.

In Fig.6, we show the complete representation, including the edges. We divide the representation into four different graph representations for simplicity. In practice, each edge in the data represents the probability per action in an arbitrary coordinate order. Therefore, we have only one graph with multiple edge features. For instance, the inner edge of the top-left yellow node on Fig.6, denoted node "1", would have the value of

$$e_{1,1} = \{1, 0, 1, 0\}, \tag{20}$$

which is the value of this edge given the left, right, up, and down actions in this order.

Non deterministic edges. MDPs are sometimes non-deterministic. That means, given a state and a desired action, it is only sometimes guaranteed to succeed. We create the non-deterministic dataset variation to simulate this setup and challenge the edge attributes generation. In this dataset, the grids and the nodes are staying the same. However, the edge attributes are now continuous instead of being binary. Still, the outgoing sum of edges from a certain node must sum up to one to be a valid MDP. Further, we decided to apply the next arbitrary distribution over the edge. Denote $|e_{out}^u| = z^u$ as the number of outgoing edges. given a desired action a and nodes u, v the rate of success is: $p(v|u, a) = 1 - 0.1 \cdot z^u$. And $p(k|u, a) = 0.1$ for any other node k neighbor of u .

Dataset generator. We will provide the complete code for generating the grids and their corresponding MDPs. The generator enables control of grid size, number of ending points, and number of blocks. In addition, if these parameters are valid, the code generates only valid graphs with a start

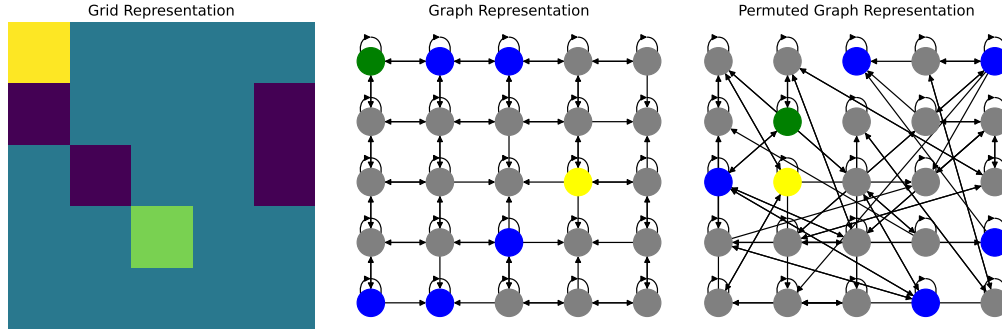


Figure 5: On the left is a grid representation of the MDP grid maze. The yellow cell is the starting point, and the ending is the green cell. The dark blue cells are blocks. In the center, a structured graph represents the grid by the rules described in the appendix. On the right, the same grid is represented by a different permutation of the nodes. Both graphs are equal, and there are $n!$ different graphs, where n is the number of nodes.

and an end. Finally, the generator gets the desired grids and randomly samples grids with the above parameters.

Dataset statistics. First, our grids are 5×5 . Second, there is only one ending point. Therefore, we have **one** starting cell and **one** ending cell. Finally, we set the number of blocks to be precisely 4. These configurations are for every grid in the dataset. We generate 1000 valid grids and split them into 80% training and 20% for testing and validations.

Evaluation protocols Besides the general graph generation metrics for directed graphs (degree and clustering), we consider several dataset-specific metrics to evaluate node and edge generation quality.

1. Edges

- (a) MDP Validity (MV): Check if the sum of the outgoing edges of a node is one. It is a constraint of an MDP that the sum of probabilities is one. In the non-deterministic setup, the values are continuous, and therefore, we use an $\epsilon = 0.01$ gap from one. Note normalization of the edges could be done to fix this constraint if necessary. However, we evaluate the hard constraint to measure the model’s ability to capture the edge feature distributions.
- (b) MDP Distribution Validity (MDV): As described before, the edge distribution is different in the non-deterministic setup. Therefore, we specifically test the model’s ability to generate edges with approximately the same distribution. Consequently, we test whether each node’s distribution we defined for the non-deterministic setup applies with an $\epsilon = 0.01$ gap.

2. Nodes

- (a) Valid Solution (VS): Measures if a generated grid is valid: has start and finish cells, and the route is not entirely blocked.
- (b) Blocks (B): Measures the absolute distance between the average number of blocks in the grids. In this work, the used dataset has a ground-truth average of four.
- (c) Start and Finish (SF): Measures the absolute distance between the average number of end and start cells; there are always exactly two in the setup we used.
- (d) Empty (E): Measures the absolute distance between the average number of regular cells.

Grid

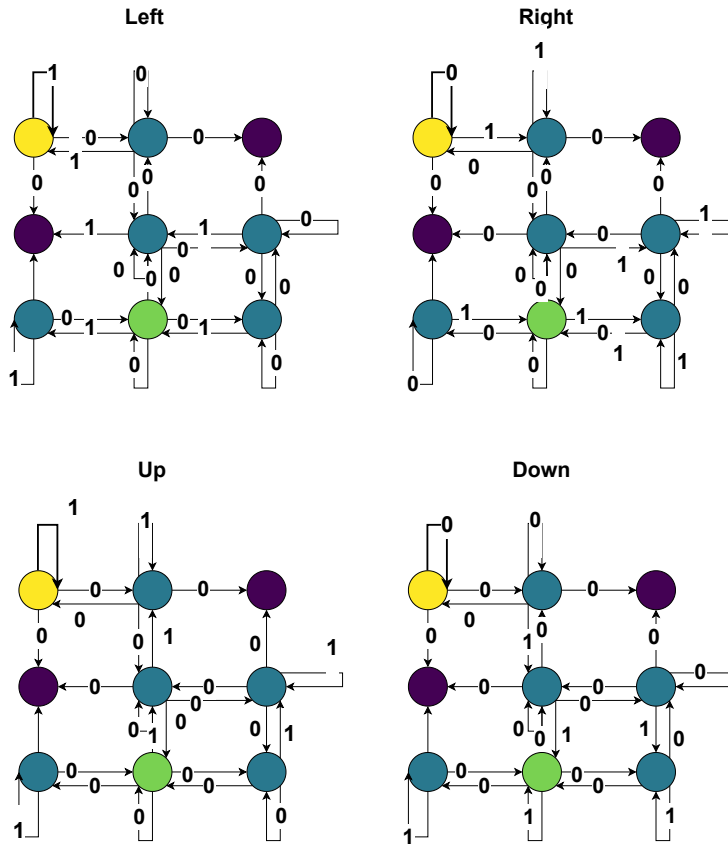


Figure 6: In the first line, a 3×3 grid example. Note that in the real dataset, the grids are 5×5 . Below, we present the four actions and show the probabilities of moving from one state to another over the edges given a specific action.

A.1.2 nuScenes Dataset

The nuScenes dataset Caesar et al. [2020] serves as a crucial resource for trajectory prediction research in autonomous driving, featuring a vast collection of real-world sensor data recorded in the urban environments of Boston and Singapore. This dataset provides essential coordinates of vehicles, lanes, and other map entities from 1000 scenes, each lasting 20 seconds, and is published at 2Hz. Primarily, it is broadly used for trajectory prediction Liu et al. [2021]. Prior works used raster representations of the scenes combined with vision-based architectures to process the rasterized image. VectorNet Gao et al. [2020] was the first to utilize a sparse graph representation of the scenes,

where nodes represent agents and map elements, which are later processed via GNNs to predict the target. It has paved the way to its graph-based successors Kim et al. [2021], Deo et al. [2022], Liu et al. [2023], now crowned as the current state-of-the-art that tops the leader-boards of this field.

Consequently, we follow their success and are convinced that such scenes can be naturally generated as graphs. For this purpose, we extract a portion of 746 samples of traffic scenarios from the *mini_train* split as defined in the nuScenes-devkit and use them for training and evaluation with 80%, 20% train, test split. Each sample is transformed into a graph with nodes of 3 types: 1. agents, with a feature vector representing an 8-second trajectory; 2. map elements, represented as x and y coordinates of their polygon; and 3. lanes, represented as discrete curves of length 8 meters each. We transform the graph into a radius graph of 30 meters and only preserve edges representing a relation whose target is an agent, e.g., lane-to-agent.

Evaluation. For evaluating the results for nuScenes graph generation, we use the standard protocol of evaluating the MMD over each node type, i.e., the x and y coordinates of the trajectories of vehicles (V), the coordinates of the lane curves (L) and other map objects (O). Additionally, we evaluate the Collision Rate (CR), which measures the rate of collisions between generated agents, and the Lane alignment (LA), which sums up the distances between each agent’s trajectory to the closest generated lane. Such a metric reflects the tendency of road participants to follow lane center lines, which is a natural behavior of road participants. We refer to Tan et al. [2021] for more details about the metrics and evaluation protocols.

A.1.3 Molecule Datasets

QM9 - The Quantum Mechanics 9 database Wu et al. [2018] contains around 130k small organic molecules with up to 9 heavy atoms and their physical properties in equilibrium, computed using density functional theory calculations. To evaluate our and other methods, we repeat the exact protocol presented in Vignac et al. [2023], Jo et al. [2022] and refer to them to learn more about the metrics and the evaluation protocols.

A.1.4 General Datasets

We present the datasets below and refer to Vignac et al. [2023] and Jo et al. [2022] for more information about the evaluation process and protocols.

- **Ego-small** - 200 small ego graphs drawn from larger Citeseer network dataset Sen et al. [2008].
- **Grid** - 100 standard 2D grid graphs. BRENDA database Schomburg et al. [2004].
- **Stochastic-Block-Model (SBM)** - This dataset comprises 200 synthetic stochastic block model graphs. These graphs have communities ranging from 2 to 5, with each community containing between 20 to 40 nodes. The probability of inter-community edges is 0.3, and intra-community edges is 0.05. Validity is determined based on the number of communities, number of nodes in each community, and a statistical test as done in Martinkus et al. [2022].
- **Planar** - This dataset comprises 200 synthetic planar graphs, each contains 64 nodes. The criteria for a valid graph within this dataset necessitate a two-fold condition: 1) the graph is connected, ensuring that every node has a path to every other node and 2) the graph must exhibit planarity, meaning you can draw it on a two-dimensional plane without any edge crossings.

A.2 Implementation Details

A.2.1 Architecture and Hyperparameters

We refer to Sec. 4 in the main text to describe the method architecture and implementation details. We present the hyperparameters per dataset in Tab. 5. We used Adam Kingma and Ba [2014] optimizer and the same learning rate of 0.01, weight decay of 0.0001, and EMA of 0.999 for all datasets. In addition, for sampling, we used the Euler predictor, Langevin corrector, signal-to-noise-ratio (SNR) of 0.05, scale epsilon of 0.7, and sampling with 1000 steps for all datasets. Finally, we use a single

Table 5: Hyperparameters for each dataset.

	Hyperparameter	MDP	MDP-non-det	nuScene	QM9	Planar	SBM	Ego	Small	Grid
Module	Attention layers	5	5	3	3	4	4	5	4	
	Edges channels	4	2	1	2	2	2	2	2	
	Initial channels	1	1	1	1	1	1	1	1	
	Hidden channels	8	8	8	8	8	8	8	8	
	Final channels	4	4	4	4	4	4	4	4	
	Attention Heads	4	4	4	4	4	4	4	4	
	Hidden dimension	32	32	32	16	32	32	32	32	
Training	Batch size	256	256	128	1024	64	26	128	7	
	Epochs	5000	5000	5000	400	5000	5000	5000	5000	
SDE	β_{min}	0.1	0.1	0.1	0.1	0.1	0.1	0.1	0.1	
	β_{max}	3	3	2	1	1	1	1	1	

VP forward diffusion process Song et al. [2021] stochastic differential equation for both the nodes and the edges. We refer Jo et al. [2022] for more details about each hyperparameter. We will publish the complete code, including the datasets, evaluation protocols, and experiment environment upon acceptance.

A.2.2 GDSS-E Baseline Implementation Details

GDSS Jo et al. [2022] is a state-of-the-art method for graph generation. However, none of the other methods are adapted to generate multiple continuous edge features and directed graphs. Therefore, to create a solid baseline for directed, multi-edge attribute graph datasets, we create an extension of GDSS called GDSS-E.

Directed graphs. To adapt GDSS to a directed graph, we need to delete the symmetry inductive bias of the method. First, we deleted the symmetry inductive biases in the attention module of the backbone architecture. In addition, the generated noise and the whole diffusion process are set to be symmetric, meaning they generate symmetric noise patterns. Therefore, we change all aspects of the diffusion and generation process to be a normal Gaussian injection, similar to regular diffusion methods.

Multiple edge features We need to enable the model to generate multiple features technically. GDSS outputs an adjacency matrix $A \in \mathbb{R}^{N \times N}$ where N is the number of nodes. We adjust the network parameter to return $E \in \mathbb{R}^{N \times N \times C}$ where the first feature is the adjacency information, and the rest of the channels are the attributes of the edges. We will publish this implementation code in the project code.

A.2.3 Permutation equivariance and invariance

Niu et al. [2020] show that if the neural backbone of a generative model is permutation equivariant, then the learned distribution by the model will be permutation invariant. This trait is essential for graph datasets since we ideally want an equal probability of sampling different permutations of the same graph. Following our model architecture, all our arithmetic actions are edge-wise, node-wise, or GNN-wise. Therefore, we preserve the permutation equivariance of the neural backbone model.

Yan et al. [2023] show that equivariance can be violated but restored with a specific invariant sampling technique. However, their study discovers one main drawback that our and other permutation equivariant models do not suffer from. The drawback is that if graphs in the observed dataset have few permuted representations, it significantly damages the model generation quality. They showed on a synthetic dataset that if there are $\approx 0.01\%$ permuted representations, their model fails to learn the distribution. On the other hand, they show that equivariant models are indeed, as expected theoretically, robust for such cases.

Table 6: General graphs datasets evaluation. ‘*’ means out of computation resources.

Method	Planar			SBM			Ego Small			Grid		
	deg↓	cl↓	orb↓	deg↓	cl↓	orb↓	deg↓	cl↓	orb↓	deg↓	cl↓	orb↓
SPECTRE	1.42	1.35	1.33	2.12	1.37	0.51	0.046	0.14	0.73	*	*	*
GraphVAE	0.87	1.13	0.83	1.41	0.97	0.52	0.13	0.23	0.052	1.48	0	0.87
EDP-GNN	0.985	1.29	0.97	1.1	1.43	0.88	0.062	0.097	0.009	0.45	0.32	0.51
DiGress	1.36	0.97	1.47	1.16	1.32	1.16	0.12	0.17	0.035	0.87	0.03	1.28
GDSS	0.945	0.96	0.66	0.74	1.57	0.25	0.025	0.087	0.015	0.37	0.01	0.42
Our w.o. edge features	0.032	0.71	0.34	0.47	1.1	0.05	0.02	0.043	0.052	0.07	0.012	0.45
Our	0.025	0.38	0.23	0.46	0.63	0.04	0.02	0.036	0.046	0.01	0.007	0.39

B Additional Experiments

B.1 Graph Benchmarks

Although we do not claim to have a superior distribution estimation for graphs where edge features are not dominant, and, in addition, our method is designed for directed graphs in contrast to all other methods, in the following two experiments, we compare our model to strong baselines on regular graph benchmarks. The generated edge features we use are arbitrary, and incorporating other engineered features on the edges, such as spectral features, could further improve our model. However, this is not our primary focus, and we leave such exploration for future research.

B.1.1 General Graphs Benchmarks

To leverage the edge attributes ability of our model, we augment every graph with edge attributes per edge. Specifically, we compute the n -th power of the adjacency matrix, and then, for each edge e_{ab} between nodes a and b , we assign the corresponding value encoded in the power matrix. The edge features contain the number of paths between a and b with n steps, where we set $n = 2$.

We compare our method with strong graph generation baselines: SPECTRE Martinkus et al. [2022], GraphVAE Simonovsky and Komodakis [2018], EDP-GNN Ho et al. [2020], DiGressVignac et al. [2023], and GDSS Jo et al. [2022]. We follow the training and evaluation protocols detailed in Jo et al. [2022], Vignac et al. [2023]. We present the results in Tab. 6. Our model achieves state-of-the-art performance in several cases. In particular, in complex and large graphs such as SBM, Planar, and Grid, our method is a strong competitor in terms of the *degree* metric compared with other methods. These results show that our method is capable of learning complex graph structures. Moreover, we report our results with standard deviation in App. 12 to show the robustness of our model. In addition, to make a fair comparison, we executed the benchmark with our model, excluding edge features. Our method achieves slightly lower results when edge features are not utilized. However, it still surpasses other methods in general.

B.1.2 Molecule Graph Benchmark

QM9: molecule generation. We additionally consider the QM9 dataset Wu et al. [2018] that contains edge types and node features of atoms of molecules. We refer the reader to App. A.1.3 to learn about the dataset, evaluation protocol, and metrics. We report in Tab. 7 the results of our evaluation in comparison to GDSS and DiGress. Importantly, we emphasize that DiGress is explicitly designed to handle the generation of edge types as it leverages transition kernels. Nevertheless, our method shows strong results, achieving the best scores on the validity w/o (Val w/o) and Uniqueness (Uni) metrics.

B.2 General Graphs Ablation Study Cont.

We extend the ablation study over the general graph benchmarks presented in Sec.5.4 and report the results in Tab.8. The results supports the claimed contributions of our model components, as presented in the main text.

Table 7: Molecule QM9 dataset.

Method	Val w/o↑	Uni↑	FCD↑	NSPDK↓
GDSS	93.2%	94.6%	2.9	0.003
DiGress	95.5%	94.1%	0.578	0.0009
Our	96.7%	95.2%	3.6	0.006

Table 8: Ablation study of our four variants of our model on four different datasets.

Method	Ego Small			Grid		
	deg↓	cl↓	orb↓	deg↓	cl↓	orb↓
GDSS-E	0.141	0.352	0.171	0.37	0.01	0.42
Joint-SDE-Model	0.063	0.167	0.062	1.8	0	1.44
GNM-Based-Model	0.021	0.038	0.048	0.49	0.006	0.51
Ours	0.04	0.02	0.036	0.046	0.01	0.007

B.3 Standard Deviation in Experiments

We present the results of the quantitative evaluations with standard deviation to emphasize our method’s robustness. We show the MDP deterministic setting in Tab. 9. We show the MDP non-deterministic setting in Tab. 10. In Tab. 11, we show nuScenes. In Tab. 12, we show the general graphs experiment with standard deviation.

Table 9: Deterministic MDPs with standard deviation.

Method	deg ↓	cl ↓	MV ↑	VS ↑	B ↓	SF ↓	E ↓
GDSS-E	0.73 ± 0.025	0.06 ± 0.002	$34\% \pm 1\%$	$9\% \pm 2\%$	0.96 ± 0.16	1.28 ± 0.05	2.23 ± 0.16
Our	0.17 ± 0.02	0.006 ± 0.001	$68\% \pm 1\%$	$34\% \pm 4\%$	0.1 ± 0.04	0.58 ± 0.13	0.48 ± 0.18

Table 10: Non deterministic MDPs with standard deviation. The top row displays the GDSS-E model, while the bottom row depicts our model

deg ↓	cl ↓	MV ↑	MDV ↑	VS ↑	B ↓	SF ↓	E ↓
0.40 ± 0.02	0.02 ± 0.01	$6\% \pm 1\%$	$1\% \pm 0.5\%$	$26\% \pm 2\%$	0.39 ± 0.03	0.83 ± 0.1	0.4 ± 0.1
0.31 ± 0.01	0.01 ± 0.001	$38\% \pm 2\%$	$6\% \pm 0.5\%$	$33\% \pm 1\%$	0.02 ± 0.02	0.88 ± 0.1	0.8 ± 0.01

Table 11: Quantitative metrics on nuScenes with standard deviation.

Method	deg ↓	cl ↓	V ↓	O ↓	L ↓	CR ↓	LA ↓
GDSS-E	1.05 ± 0.1	0.03 ± 0.003	3.9 ± 0.19	0.66 ± 0.13	0.96 ± 0.14	0.5%	208 ± 21
Our	0.77 ± 0.08	$6e^{-7} \pm 4e^{-7}$	0.36 ± 0.01	0.8 ± 0.1	0.08 ± 0.03	0.3%	194 ± 15

Table 12: General graph datasets evaluation with standard deviations of our method

Dataset	degree ↓	cluster ↓	orbit ↓
Planar	0.025 ± 0.009	0.38 ± 0.06	0.23 ± 0.005
SBM	0.46 ± 0.09	0.63 ± 0.04	0.05 ± 0.0001
Ego Small	0.02 ± 0.011	0.036 ± 0.0087	0.046 ± 0.0073
Grid	0.01 ± 0.003	0.007 ± 0.001	0.39 ± 0.07

B.4 Graphs Visualizations Generated by Our Model

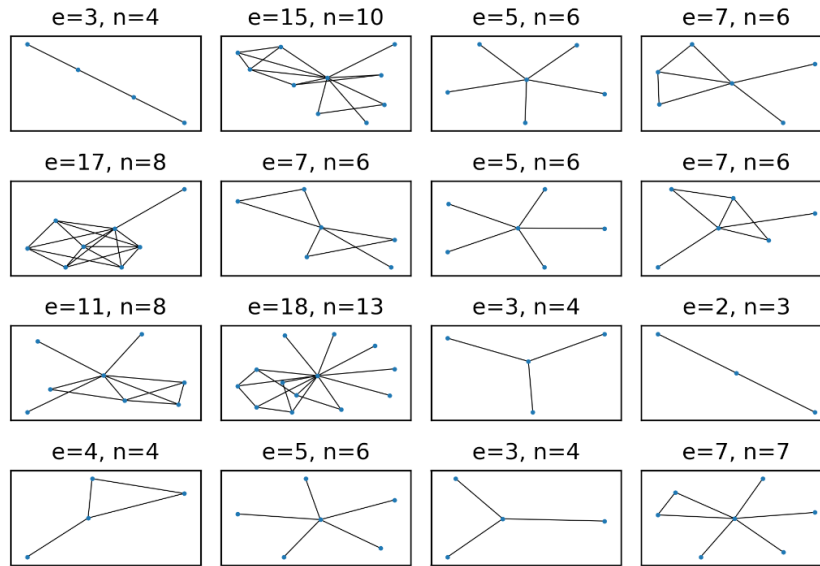


Figure 7: General graphs - Ego Small

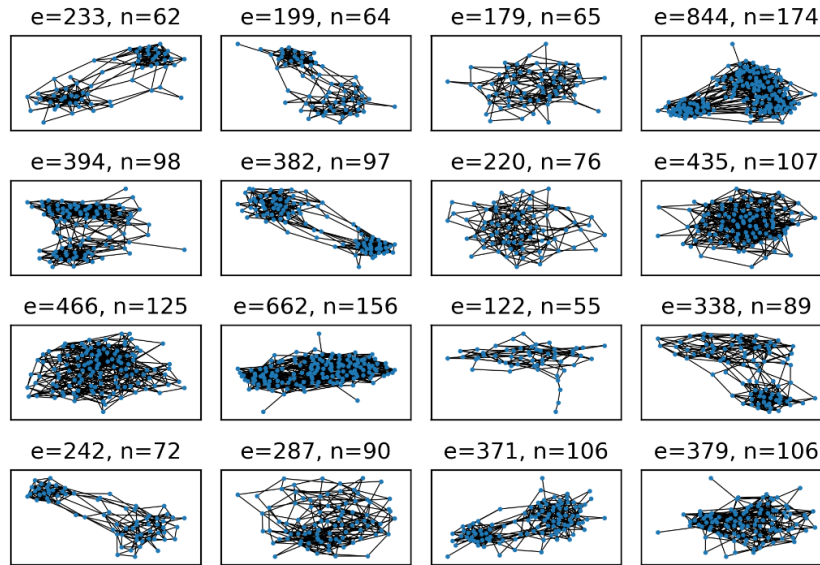


Figure 8: General graphs - SBM

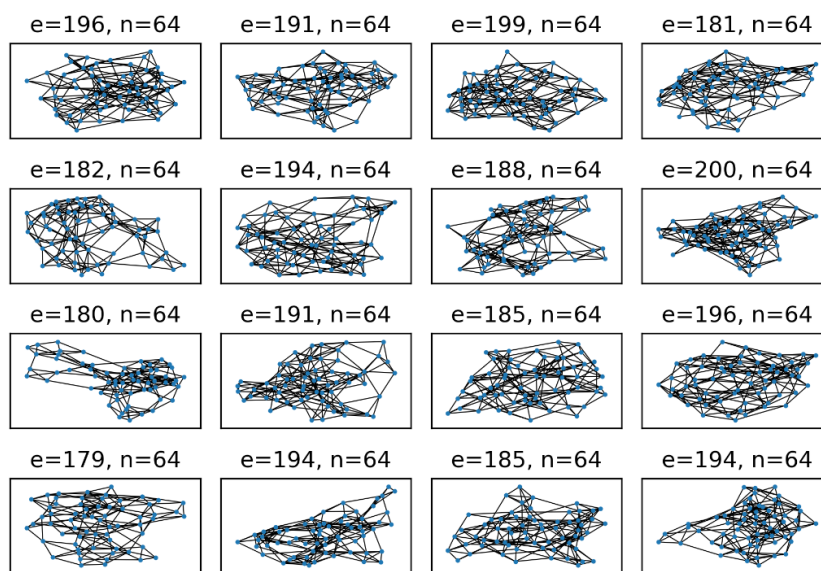


Figure 9: General graphs - Planar

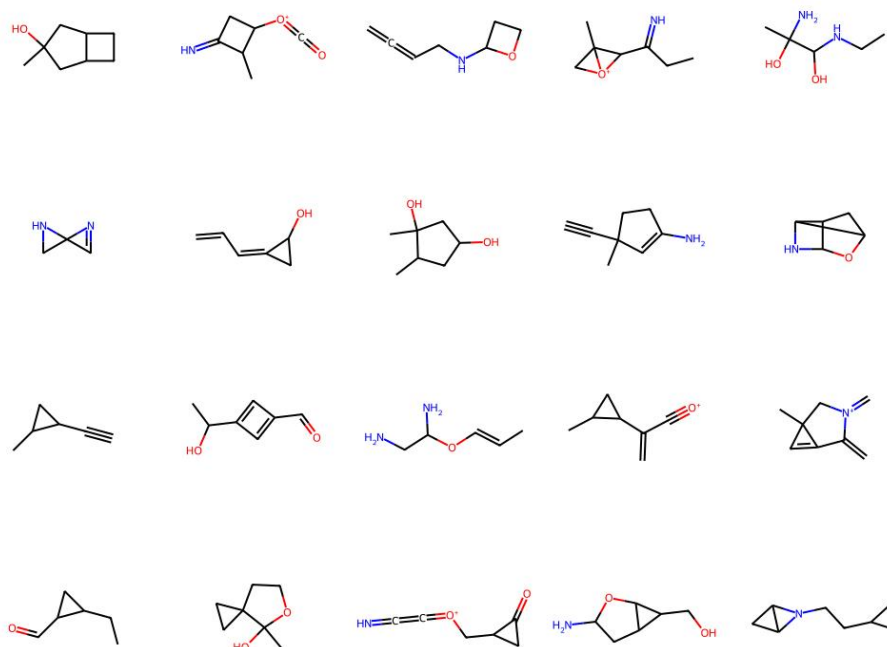


Figure 10: Molecule Graphs - QM9